HHS Public Access

Author manuscript

FEBS J. Author manuscript; available in PMC 2017 November 01.

Published in final edited form as:

FEBS J. 2016 November ; 283(21): 3889–3897. doi:10.1111/febs.13906.

Atg1-independent induction of autophagy by the Drosophila Ulk3 homolog, ADUK

Christopher R. Braden and **Thomas P. Neufeld***

Department of Genetics, Cell Biology and Development, University of Minnesota, 6-160 Jackson Hall, 321 Church St. SE, Minneapolis, MN 55455 USA

Abstract

Although canonical autophagy regulation requires a multi-protein complex centered on the Ser/Thr-kinase Atg1 (mammalian Ulk1/2), alternative signals can induce autophagy independently of Atg1 through unknown mechanisms. Here we identify the Drosophila Ulk3 ortholog, ADUK, as an Atg1-independent autophagy inducer. ADUK interacts with Atg1 complex members Atg13 and Fip200, and requires Atg13 but not Atg1 for autophagy induction. Loss of ADUK shortens adult lifespan and reduces the autophagic response to a chemical stressor, DMSO. However, ADUK is not required for autophagy induction by Atg1-dependent nutrient or developmental cues. Atg1 and ADUK/Ulk3 thus represent alternative catalytic components of a shared autophagy kinase complex.

Graphical abstract

*Corresponding author. neufe003@umn.edu, Tel: 612-625-5158, Fax: 612-626-5652.

Author Contributions

The project was initiated by TPN. Experiments were planned by CRB and TPN. Experiments were performed and data was analyzed by CRB. The paper was written by CRB and revised by TPN.

Conflict of Interest

The authors declare no conflict of interest.

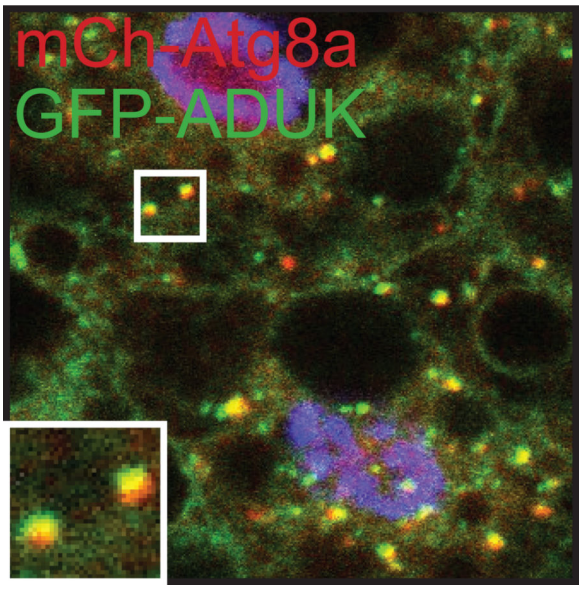

Atg1/Ulk1-independent autophagy has been previously reported, but the mechanisms remain elusive. Here we identify the Drosophila Ulk family kinase ADUK as an Ulk3 ortholog that can promote autophagy in the absence of Atg1, through interactions with FIP200 and Atg13. Despite sharing these factors with Atg1, ADUK is dispensable for starvation-induced autophagy, but is required for autophagy induction by chemical stress.

Keywords

autophagy; non-canonical; Ulk1; Ulk3; Atg1; Atg13; Drosophila

Introduction

Macroautophagy (hereafter autophagy) is the process of sequestering cellular components, including protein, protein aggregates, and organelles, for transport to the lysosome and subsequent destruction. Sequestration is accomplished by the formation of a specialized double-membrane bound vesicle known as the autophagosome. Formation, maturation, and lysosomal fusion of the autophagosome are tightly regulated, as both excessive and insufficient autophagy can result in negative consequences to homeostasis.

Nutrient status is perhaps the best known and most well-studied stimulus resulting in autophagy modulation, and is mediated by the interaction of the pro-growth mechanistic target of rapamycin complex I (mTORC1) and a pro-autophagy complex centered around the serine/threonine kinase Atg1 (Unc51-like kinase [Ulk]1 and Ulk2 in mammals) and its binding partners Atg13, Atg101 and FIP200 (1-3). Insulin signaling and amino acid supply are integrated at mTORC1, resulting in activation of mTOR kinase (4). In response, mTORC1 blocks unnecessary autophagy by phosphorylating and thereby inhibiting the activity of the Atg1 complex (5-7).

While Atg1 and its homologs Ulk1/2 are crucial for autophagy induction during starvation, recent work in various model systems has identified stimuli capable of inducing autophagy in their absence (2, 8, 9). How these signals engage the autophagy machinery independent of this kinase complex is poorly understood. Of note, a third Unc51-like kinase, Ulk3, has been linked to senescence, Hedgehog signaling, and cytokinesis in mammalian cells (10-12), but its role in autophagy remains largely uncharacterized. Here we examine the role of the Drosophila Ulk3 ortholog, which we have named “Another Drosophila Unc-51-Like Kinase” (ADUK). We find that ADUK represents an Atg1-independent pathway to autophagy induction that nonetheless requires Atg13. ADUK interacts physically with Atg13 and genetically with the Atg1-Atg13 binding partner FIP200. Loss of ADUK reduces adult survival and blunts the autophagic response to a complex stressor, but has no effect on autophagy induction in response to known Atg1-dependent stimuli. We propose a model in which separate upstream pathways regulate one of two similar autophagy initiating complexes, both containing Atg13 but differing in the use of either Atg1 or ADUK/Ulk3 as a kinase effector.

Results & Discussion

While considering possible mechanisms for Atg1-independent autophagy regulation, we identified the mammalian protein Ulk3 as a strong candidate for its Atg1-family kinase domain and ability to induce accumulation of autophagic markers in cell culture (10). We then sought to identify non-mammalian homologues, and found that unstudied gene CG8866 in *Drosophila melanogaster* encodes a protein with similar predicted kinase and MIT (microtubule interacting and trafficking motif) domains (**Figure 1A**). Phylogenetic analysis of Ulk family genes from Saccharomyces cerevisiae, Caenorhabditis elegans, Drosophila, and humans confirms that CG8866 is most closely related to mammalian Ulk3 (Figure 1B). To examine the effect of CG8866 (hereafter “ADUK”) on autophagy in *Drosophila*, we generated transgenic lines capable of overexpressing ADUK. To detect autophagic vesicles, we co-expressed mCherry-tagged Atg8a, an ubiquitin-like molecule that labels the membranes of autophagosomes and autolysosomes. Clonal overexpression of ADUK in the fat body of well-fed *Drosophila* larvae led to accumulation of mCherry-Atg8a punctae, whereas autophagy was limited to basal levels in surrounding control cells (**Figure 1C-C”**).

An increase in the number of autophagic vesicles can be indicative of either autophagy induction or a late-stage block in autophagosome-lysosome fusion or acidification, leading to an accumulation of early or defective structures with no means of turnover (13, 14). We therefore asked whether autophagosomes colocalized with lysosomes and whether autolysosome acidification was intact in ADUK-expressing cells, both necessary steps in the formation of functional autolysosomes. ADUK-induced mCherry-Atg8a punctae did indeed co-localize with the lysosomal marker LAMP1-GFP (**Figure 1D-D”**). Use of the acidic compartment dye Lysotracker showed normal development of acidic vesicles in ADUK overexpression clones (**Figure 1E-E”**), consistent with formation of autolysosomes during autophagy (15). To further explore the possibility of a late stage block, we tested the effect of ADUK overexpression during a stimulus known to induce autophagy, amino acid starvation. During starvation-induced autophagy, a downstream block in autophagosome maturation or turnover results in excessive size and number of autophagosomes (16).

However, clonal overexpression of ADUK in starved animals did not perturb the appearance of autophagosomes compared with those in wild-type neighboring cells (**Figure 1F-F”**), suggesting that a block in turnover is not the reason for ADUK-induced mCherry-Atg8a punctae. Together, these results indicate that ADUK overexpression leads to an increase in the number of autophagic vesicles by inducing autophagy, rather than by blocking progression of basal autophagy.

To monitor the sub-cellular localization of ADUK, we generated a GFP-tagged ADUK transgene. Interestingly, in both fed and starved animals, GFP-ADUK localized to punctate structures throughout the fat body, most of which colocalized with or adjacent to mCherry-Atg8a labeled vesicles (**Figure 1G-G”**). Thus, ADUK both induces and localizes to autophagic vesicles, as described for other Ulk-family kinases (1, 3, 10, 17).

As we initially set out in search of Atg1-independent mechanisms, we next tested the requirement for Atg1 in ADUK-induced autophagy. Null mutation of Atg1 has been shown to block autophagy induction in response to starvation and developmental cues in the larval fat body. Interestingly, clonal overexpression of ADUK in the fat bodies of Atg1-null mutant animals led to a robust formation of mCherry-Atg8a punctae in both fed and starved conditions (**Figure 2A-A”**), indicating that autophagy was induced by ADUK expression despite a lack of Atg1. To further explore the relationship between Atg1 and ADUK, we examined the effect of ADUK on Atg1-induced phenotypes in the *Drosophila* eye. Atg1 overexpression in the eye results in reduced area (17), a phenotype that can be suppressed by depleting FIP200 (**Figure 2E**). Because ADUK and Atg1 overexpression each induce autophagy, we expected co-expression of ADUK would enhance the Atg1 reduced-eye phenotype. Surprisingly, co-expression of ADUK with Atg1 significantly suppressed the Atg1-induced eye size reduction phenotype (**Figure 2E**). This suggests that rather than enhancing Atg1-induced autophagy, ADUK either opposes Atg1 or competes for binding partners, thereby blunting the response to Atg1 overexpression. To test for competition between ADUK and Atg1, we attempted to block ADUK overexpression-induced autophagy in the fat body by co-expressing a dominant negative, kinase-defective Atg1. This ablated the autophagic response to ADUK overexpression (**Figure 2B&C**), suggesting that dominant negative Atg1 is capable of interfering with factors necessary for ADUK-induced autophagy. Together, our results indicate that ADUK promotes autophagy independently of Atg1 and that these kinases potentially share required regulatory factors.

One of the best characterized Atg1 binding partners is Atg13, a structural protein required for starvation-induced autophagy. To ask whether autophagy induction by ADUK requires Atg13, we overexpressed ADUK in Atg13 mutant larvae. In contrast to its effects in Atg1 mutant and wild type control cells, ADUK overexpression in Atg13 mutant cells did not lead to autophagy induction (**Figure 2D-D”**), indicating that the function of Atg13 is required either together with or downstream of ADUK.

The ability of ADUK to induce autophagy in the absence of Atg1, but not in the absence of Atg13 or the presence of a dominant negative Atg1, is consistent with ADUK competing with Atg1 for binding to Atg13. Although Atg1/Ulk1 and ADUK/ULK3 share no apparent sequence identity beyond their kinase domains, the C terminal region of both proteins

contains structurally similar MIT domains that in the case of yeast Atg1 and mammalian Ulk1 have been shown to be required for Atg13 binding (18-20). To ask whether ADUK and Atg13 form a complex *in vivo*, we tested whether tagged versions of these proteins could interact by co-immunoprecipitation. As previously reported (2), Atg13-Flag readily co-immunoprecipitated with GFP-Atg1 from whole animal extracts (**Figure 2F**). Similarly, GFP-ADUK was capable of pulling down Atg13-Flag. Interestingly, whereas overexpression of Atg1 led to phosphorylation and reduced gel migration of Atg13 as previously shown (2), ADUK overexpression did not effect the migration properties of Atg13 **(Figure 2F, input)**.

To further explore the relationship between ADUK and Atg1 complex members, we examined the effects of Atg13 and FIP200 co-expression on ADUK overexpression phenotypes. Atg1-dependent autophagy has previously been shown to be enhanced by co-expression of Atg13 or FIP200 (2, 3). Similarly, co-expression of FIP200 with GFP-ADUK significantly enhanced the formation of both GFP-ADUK (**Figure 3B**) and mCherry-Atg8a punctae (**Figure 3B'**). In contrast, co-expression of Atg13 with GFP-ADUK suppressed GFPADUK and mCherry-Atg8a punctae formation (**Figure 3C and C'**). Together, these results suggest that ADUK and Atg1 enter into complexes with a shared set of proteins but likely differ significantly in their regulatory interactions.

The findings that ADUK induces autophagy Atg1-independently, interacts with Atg1 binding partners, and bears a similar kinase domain to Atg1 are consistent with ADUK representing a parallel pathway to Atg1, converging at the level of Atg13 and FIP200. It is also possible, however, that ADUK acts downstream of Atg1 in a second complex requiring similar elements. To distinguish these possibilities and to further explore the role of ADUK during autophagy, we generated an ADUK deletion allele by imprecise P-element excision. The deletion, Δ3b, eliminates 705 nucleotides of the ADUK gene (**Figure 4A and Supplemental Figure S1**). This includes the majority of the conserved kinase domain of ADUK, including the ATP-binding pocket, and creates a frame-shift leading to a premature stop after 6 codons. $ADUK^{\Delta 3b}$ homozygotes demonstrated no obvious defects, although mutant survival post-eclosure was reduced compared with wild-type animals (**Figure 4B**).

$ADUK^{\Delta 3b}$ mutant clones displayed no ectopic autophagy under non-stressed conditions, consistent with the pro-autophagy role demonstrated by overexpression (data not shown). ADUK mutants also displayed normal autophagosome formation in response to amino acid starvation (**Figure 4C-C"**) and during wandering phase developmental autophagy (**Figure 4D-D"**), both Atg1-dependent autophagy stimuli. Thus ADUK is not required downstream of Atg1, further supporting that these kinases act in parallel.

If ADUK represents an Atg1-independent parallel mechanism for engaging the autophagic machinery, ADUK may either represent a redundant Atg1-like protein or an effector required for autophagy in response to a different stimulus or set of stimuli. Of several potential alternative autophagy stimuli examined, we found that ADUK was required for induction of autophagy in response to the amphipathic solvent DMSO, which was recently shown to decrease triglyceride accumulation through induction of autophagy in hepatocytes (21). Subjecting larvae to DMSO-containing food induced autophagy in wild type fat body cells, and this response was blunted in both ADUK and Atg1 mutant clones (**Figure 4E-E"**

and data not shown). DMSO has been shown to have diverse effects on Ca^{2+}-dependent signaling, nucleotide metabolism and global patterns of transcription and protein phosphorylation, suggesting that its effects on autophagy are likely complex (22-24). Overall, the finding that ADUK is involved in autophagy induction in a manner that cannot be compensated for by Atg1 alone demonstrates that these kinases can function non-redundantly and in parallel to activate autophagy in response to distinct cues.

Up to now no mechanism for plausibly circumventing Atg1 has been demonstrated. ADUK and potentially its mammalian counterpart Ulk3 represent an appealingly simple method for sidestepping the requirement for Atg1 during autophagy induction. Our data show that ADUK is capable of inducing autophagy even in the absence of Atg1, and furthermore that it requires and physically interacts with Atg13. ADUK phenotypes are also enhanced by co-expression of Atg1 binding partner FIP200. Thus ADUK, which shares a kinase domain with Atg1, may simply supplant Atg1 in the autophagy initiation complex and regulate similar downstream targets. Notably, it was recently shown that autophagy induction in DT40 lymphoma cells requires Atg13 but not Ulk1 or Ulk2, suggesting that the promiscuity of Atg13 is conserved (8).

Though ADUK appears to fulfill the duties of Atg1 in autophagy induction, its relationship with Atg13 seems more complex. Co-expression of Atg1 with Atg13 hyperactivates autophagy and increases Atg13 phosphorylation, but neither is observed during ADUK and Atg13 co-expression. While the consequences of Atg13 phosphorylation are poorly understood, the inhibition of starvation- and ADUK-induced autophagy by Atg13 overexpression suggests that ADUK may be a less potent activator than Atg1, or that another activating signal may be required at the level of Atg13 for ADUK-induced autophagy to progress. Alternatively, Atg13 might sequester binding partners necessary for ADUK-induced autophagy in a way that isn't relevant to Atg1-induced autophagy. In either case, this difference in behavior highlights a key difference between ADUK- and Atg1-induced autophagy.

Mammalian cell culture work on Ulk3 has yielded an interesting pair of papers establishing a role for the kinase in the Hedgehog signaling pathway, where it acts as a homologue to the Drosophila Fused kinase by phosphorylating and promoting the nuclear translocation of Gli transcription factors (11, 25). This is of potential relevance to our work, as a link between Hedgehog signaling and autophagy exists in both mammalian and *Drosophila* models (26). However, active Hedgehog signaling inhibits autophagy, meaning that mammalian Ulk3's roles as both pro-Hedgehog and pro-autophagy conflict and may represent separate populations of the kinase. Furthermore, we observed no obvious cell growth modulation, developmental timing change, or morphological defects in *Drosophila* ADUK mutant or overexpression lines (data not shown), making it unlikely that ADUK plays a major role in the *Drosophila* Hedgehog signaling pathway.

We submit that ADUK induces autophagy by a novel type of Atg1-independent mechanism, likely replacing Atg1 in the canonical autophagy-initiation complex containing Atg13 and FIP200 to engage autophagic machinery.

Methods

Drosophila Stocks and Genetic Manipulations

Flies were raised at 25°C on standard cornmeal/molasses/agar media. The following *D. melanogaster* strains were used: UAS-mCherry-Atg8a, UAS-Atg13 and Atg13 [Δ81] (2), UAS-LAMP- GFP (gift of Helmut Krämer, University of Texas, Dallas, TX), *Atg1[Δ3D]* (15), UAS-Atg1[GS10797] and UAS-Atg1[K38Q] (17). Additional strains were obtained from the Bloomington Drosophila Stock Center (Bloomington, IN).

Deletions in the *CG8866/ADUK* locus were generated by imprecise excision of P element CG8866[EY18321], inserted 14 bases downstream of the annotated *CG8866* translation start site. Potential deletions were screened by PCR and confirmed by sequence analysis.

Loss- or gain-of-function genetic clones were induced in larval fat body through heat shock-induced or spontaneous recombination as described (2).

Transgenic Lines

UAS-ADUK—Drosophila *ADUK* cDNA GM08204 (DGRC, Bloomington, IN) was amplified with flanking Not1 and Xba1 sites and ligated into pUAST.

UAS-GFP-ADUK—The *ADUK* coding sequence was amplified from cDNA GM08204 with flanking *attB* sites, recombined into pDONOR 221 (Invitrogen, Carlsbad, CA), and subsequently recombined into pTGW (DGRC).

Survival

For each genotype, 10 male and 10 female freshly-eclosed adults were collected over an 8h period and added to each of 5 separate vials (100 total animals/genotype) containing fly media. Survivors were counted and transferred to fresh media daily.

Histology and Imaging

For starvation and DMSO treatments, larvae were collected 72h after egg laying, raised in fresh fly media under uncrowded conditions for 16–24 h, then transferred to treatment conditions: Starvation - 20% sucrose solution for 4h before dissection; DMSO - 5% DMSO in fresh fly media for 5h before dissection. For developmental autophagy, wandering larvae were collected 120h after egg laying. LysoTracker Red (Invitrogen) staining of live fat body was performed as described (27). Confocal imaging of GFP- and mCherry-tagged proteins was performed on fixed fat body tissues as described (2). Images were further processed with ImageJ (NIH, Bethesda, MD) or Photoshop CS5 and assembled into figures using InDesign CS5 (Adobe, San Jose CA). For punctae number analysis, nuclear regions were eliminated using Photoshop CS5 to restrain the analysis to the cytosol. Punctae were counted with the Analyze Particles feature in ImageJ.

Phylogenetic Analysis

Phylogenetic tree was generated by input of FASTA peptide sequences into phylogeny.fr (www.phylogeny.fr) using the One Click protocol (28-34).

Immunoprecipitation and Western Blot Analysis

hsGAL4-mediated expression of GFP-ADUK, GFP-Atg1 and Flag-Atg13 was induced in 72–96h larvae by 2h heat shock at 37°C, followed by 3h recovery under wellfed conditions. 30 carcasses per genotype were lysed in 500 μl ice-cold extraction buffer, cleared, and incubated at 4°C for 1h with anti-GFP nanobody-linked agarose gel beads (Allele Biotech, San Diego, CA) according to the manufacturer's instructions. Immunoblotting was performed as described (2) using mouse anti-Flag M5 1:10,000 (Sigma-Aldrich, St. Louis, MO) and rabbit anti-GFP ab6559 (abcam, Cambridge, MA) 1:15,000.

Supplementary Material

Refer to Web version on PubMed Central for supplementary material.

Acknowledgements

We would like to thank undergraduate research assistants Mandy Chan and Alex Sarkis for their assistance with work on the modulation of ADUK phenotypes. This work was supported by NIH grant R01 GM62509 to TPN.

Abbreviations

ADUK	Another Drosophila Unc-51-like kinase
Atg	Autophagy related
DMSO	Dimethyl sulfoxide
FIP200	Focal adhesion kinase family interacting protein 200
GFP	Green fluorescent protein
LAMP1	Lysosome associated membrane protein 1
TOR	Target of rapamycin
TORC	TOR complex
Ulk	Unc-51-like kinase
Unc	Uncoordinated

References

1. Noda NN, Fujioka Y. Atg1 family kinases in autophagy initiation. Cell Mol Life Sci. 2015
2. Chang YY, Neufeld TP. An Atg1/Atg13 complex with multiple roles in TOR-mediated autophagy regulation. Mol Biol Cell. 2009; 20(7):2004–14. [PubMed: 19225150]
3. Nagy P, Karpati M, Varga A, Pircs K, Venkei Z, Takats S, et al. Atg17/FIP200 localizes to perilysosomal Ref(2)P aggregates and promotes autophagy by activation of Atg1 in Drosophila. Autophagy. 2014; 10(3):453–67. [PubMed: 24419107]
4. Efeyan A, Comb WC, Sabatini DM. Nutrient-sensing mechanisms and pathways. Nature. 2015; 517(7534):302–10. [PubMed: 25592535]

5. Jung CH, Jun CB, Ro SH, Kim YM, Otto NM, Cao J, et al. ULK-Atg13-FIP200 complexes mediate mTOR signaling to the autophagy machinery. Mol Biol Cell. 2009; 20(7):1992–2003. [PubMed: 19225151]
6. Wong PM, Puente C, Ganley IG, Jiang X. The ULK1 complex: sensing nutrient signals for autophagy activation. Autophagy. 2013; 9(2):124–37. [PubMed: 23295650]
7. Dunlop EA, Tee AR. mTOR and autophagy: a dynamic relationship governed by nutrients and energy. Semin Cell Dev Biol. 2014; 36:121–9. [PubMed: 25158238]
8. Alers S, Loffler AS, Paasch F, Dieterle AM, Keppeler H, Lauber K, et al. Atg13 and FIP200 act independently of Ulk1 and Ulk2 in autophagy induction. Autophagy. 2011; 7(12):1423–33. [PubMed: 22024743]
9. Cheong H, Lindsten T, Wu J, Lu C, Thompson CB. Ammonia-induced autophagy is independent of ULK1/ULK2 kinases. Proc Natl Acad Sci U S A. 2011; 108(27):11121–6. [PubMed: 21690395]
10. Young AR, Narita M, Ferreira M, Kirschner K, Sadaie M, Darot JF, et al. Autophagy mediates the mitotic senescence transition. Genes & development. 2009; 23(7):798–803. [PubMed: 19279323]
11. Maloverjan A, Piirsoo M, Michelson P, Kogerman P, Osterlund T. Identification of a novel serine/threonine kinase ULK3 as a positive regulator of Hedgehog pathway. Exp Cell Res. 2010; 316(4):627–37. [PubMed: 19878745]
12. Caballe A, Wenzel DM, Agromayor M, Alam SL, Skalicky JJ, Kloc M, et al. ULK3 regulates cytokinetic abscission by phosphorylating ESCRT-III proteins. eLife. 2015:4.
13. Klionsky DJ, Abdalla FC, Abeliovich H, Abraham RT, Acevedo-Arozena A, Adeli K, et al. Guidelines for the use and interpretation of assays for monitoring autophagy. Autophagy. 2012; 8(4):445–544. [PubMed: 22966490]
14. Mauvezin C, Ayala C, Braden CR, Kim J, Neufeld TP. Assays to monitor autophagy in Drosophila. Methods. 2014; 68(1):134–9. [PubMed: 24667416]
15. Scott RC, Schuldiner O, Neufeld TP. Role and regulation of starvation-induced autophagy in the Drosophila fat body. Dev Cell. 2004; 7(2):167–78. [PubMed: 15296714]
16. Mauvezin C, Nagy P, Juhasz G, Neufeld TP. Autophagosome-lysosome fusion is independent of V ATPase-mediated acidification. Nature communications. 2015; 6:7007.
17. Scott RC, Juhasz G, Neufeld TP. Direct induction of autophagy by Atg1 inhibits cell growth and induces apoptotic cell death. Curr Biol. 2007; 17(1):1–11. [PubMed: 17208179]
18. Chan EY, Longatti A, McKnight NC, Tooze SA. Kinase-inactivated ULK proteins inhibit autophagy via their conserved C-terminal domains using an Atg13-independent mechanism. Mol Cell Biol. 2009; 29(1):157–71. [PubMed: 18936157]
19. Fujioka Y, Suzuki SW, Yamamoto H, Kondo-Kakuta C, Kimura Y, Hirano H, et al. Structural basis of starvation-induced assembly of the autophagy initiation complex. Nature structural & molecular biology. 2014; 21(6):513–21.
20. Row PE, Liu H, Hayes S, Welchman R, Charalabous P, Hofmann K, et al. The MIT domain of UBPY constitutes a CHMP binding and endosomal localization signal required for efficient epidermal growth factor receptor degradation. J Biol Chem. 2007; 282(42):30929–37. [PubMed: 17711858]
21. Song YM, Song SO, Jung YK, Kang ES, Cha BS, Lee HC, et al. Dimethyl sulfoxide reduces hepatocellular lipid accumulation through autophagy induction. Autophagy. 2012; 8(7):1085–97. [PubMed: 22722716]
22. Morley P, Whitfield JF. The differentiation inducer, dimethyl sulfoxide, transiently increases the intracellular calcium ion concentration in various cell types. J Cell Physiol. 1993; 156(2):219–25. [PubMed: 8393876]
23. Scher BM, Scher W, Robinson A, Waxman S. DNA ligase and DNase activities in mouse erythroleukemia cells during dimethyl sulfoxide-induced differentiation. Cancer Res. 1982; 42(4):1300–6. [PubMed: 6949637]
24. Faille A, Poirier O, Turmel P, Chomienne C, Charron DJ, Abita JP. Changes in the patterns of protein phosphorylation associated with granulocytic and monocytic-induced differentiation of HL-60 cells. Anticancer research. 1986; 6(5):1053–63. [PubMed: 3467646]

25. Maloverjan A, Piirsoo M, Kasak L, Peil L, Osterlund T, Kogerman P. Dual function of UNC-51-like kinase 3 (Ulk3) in the Sonic hedgehog signaling pathway. J Biol Chem. 2010; 285(39):30079–90. [PubMed: 20643644]

26. Jimenez-Sanchez M, Menzies FM, Chang YY, Simecek N, Neufeld TP, Rubinsztein DC. The Hedgehog signalling pathway regulates autophagy. Nature communications. 2012; 3:1200.

27. Juhasz G, Neufeld TP. Experimental control and characterization of autophagy in Drosophila. Methods Mol Biol. 2008; 445:125–33. [PubMed: 18425447]

28. Dereeper A, Audic S, Claverie JM, Blanc G. BLAST-EXPLORER helps you building datasets for phylogenetic analysis. BMC evolutionary biology. 2010; 10:8. [PubMed: 20067610]

29. Dereeper A, Guignon V, Blanc G, Audic S, Buffet S, Chevenet F, et al. Phylogeny.fr: robust phylogenetic analysis for the non-specialist. Nucleic Acids Res. 2008; 36(Web Server issue):W465–9. [PubMed: 18424797]

30. Chevenet F, Brun C, Banuls AL, Jacq B, Christen R. TreeDyn: towards dynamic graphics and annotations for analyses of trees. BMC bioinformatics. 2006; 7:439. [PubMed: 17032440]

31. Anisimova M, Gascuel O. Approximate likelihood-ratio test for branches: A fast, accurate, and powerful alternative. Systematic biology. 2006; 55(4):539–52. [PubMed: 16785212]

32. Edgar RC. MUSCLE: multiple sequence alignment with high accuracy and high throughput. Nucleic Acids Res. 2004; 32(5):1792–7. [PubMed: 15034147]

33. Guindon S, Gascuel O. A simple, fast, and accurate algorithm to estimate large phylogenies by maximum likelihood. Systematic biology. 2003; 52(5):696–704. [PubMed: 14530136]

34. Castresana J. Selection of conserved blocks from multiple alignments for their use in phylogenetic analysis. Molecular biology and evolution. 2000; 17(4):540–52. [PubMed: 10742046]

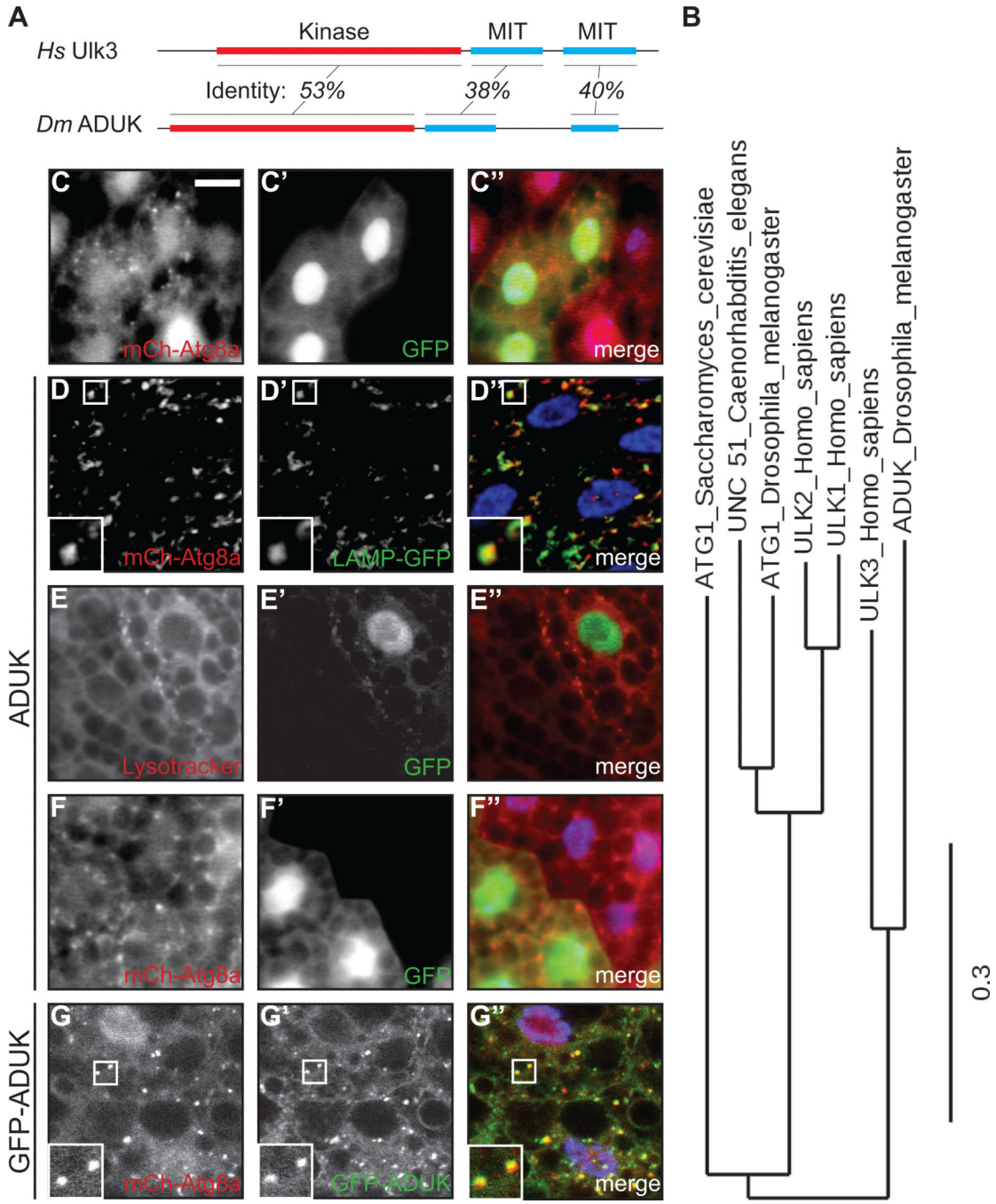

Figure 1. ADUK induces autophagy and co-localizes with autophagic markers

A: Conservation of domain composition and amino acid sequence between human Ulk3 and Drosophila ADUK. **B:** Unrooted phylogenetic analysis of selected Ulk sequences as performed by phylogeny.fr. Scale indicates proportion of variation per amino acid for corresponding branch length. Support for all branches >0.85. **C-C":** Overexpression of ADUK in GFP-marked fat body clones of well-fed animals results in mCherry-Atg8a punctae accumulation, compared with diffuse mCherry-Atg8a in neighboring control cells. **D-D''**: mCherry-Atg8a punctae co-localize with Lamp-GFP-marked lysosomes in response

to ADUK overexpression throughout the fat body of well-fed animals. Closeup of single punctum in insets. **E-E’’**: Overexpression of ADUK in GFP-marked clones induces formation of enlarged acidic vesicles under fed conditions, as indicated by Lysotracker staining. **F-F’’**: mCherry-Atg8a punctae formation in GFP-marked ADUK overexpression clone and control cells, from animals starved for amino acids. **G-G’’**: GFP-ADUK co-localizes with mCherry-Atg8a labeled autophagosomes in well-fed animals. Closeup of two punctae in insets. Nuclei counterstained with DAPI. Scale bar represents 10 μm.

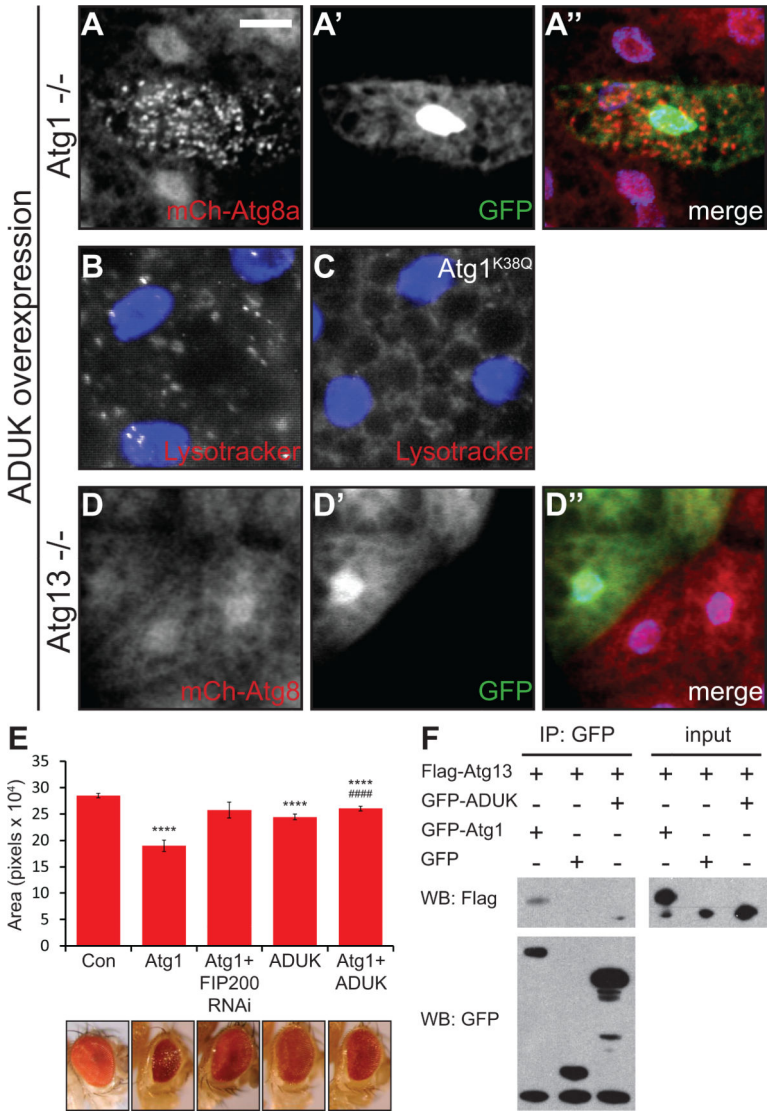

Figure 2. ADUK-induced autophagy is Atg1-independent, but requires Atg13

A-A'': Maximum intensity projection of 7 layer z-stack shows mCherry-Atg8a punctae accumulate in GFP-marked ADUK overexpression clones in well-fed animals homozygous for the $Atg1^{\Delta 3d}$ null mutation. **B&C:** ADUK-induced Lysotracker punctae formation (B) is blocked by co-expression of kinase-defective $Atg1^{K38Q}$ (C). **D-D'':** Overexpression of ADUK in GFP-marked clones does not induce mCherry-Atg8a punctae in well-fed animals homozygous for the $Atg13^{\Delta 81}$ null mutation. Nuclei counterstained with DAPI. Scale bar represents 10 μm. **E**: Adult eye area under GMR-GAL4 driven eye-specific overexpression of the indicated transgenes. Atg1+FIP200 RNAi n=7, all others n=10; **** = $p<0.00005$ vs. Con, #### = $p<0.00005$ vs. Atg1; Student's t-test. Error bars represent standard error. **F**: Flag-Atg13 co-immunoprecipitates from fat body lysates with GFP-Atg1 and GFP-ADUK but not with GFP.

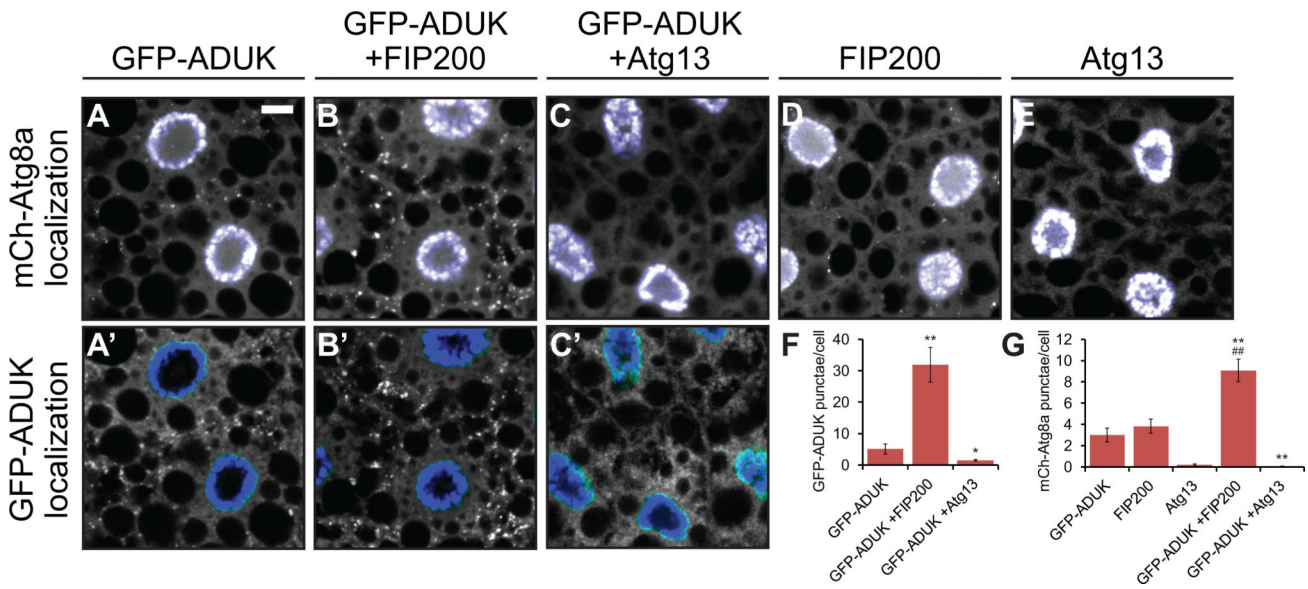

Figure 3. ADUK overexpression phenotypes are modulated by co-expression of canonical Atg1 complex members

A-E: Autophagosome formation detected by mCherry-Atg8a punctae in response to independent overexpression of GFP-ADUK (**A**), FIP200 (**D**), or Atg13 (**E**), or to co-expression of GFP-ADUK with FIP200 (**B**) or with Atg13 (**C**). **A'-C'**: GFP-ADUK punctae formation alone (**A'**) or with FIP200 (**B'**) or Atg13 (**C'**) co-expression. **F:** GFP-ADUK punctae per cell in genotypes shown in A'-C'. GFP-ADUK n=9, GFP-ADUK + FIP200 n=11, GFP-ADUK + Atg13 n= 10. * = p<0. 05, ** = p<0. 005 vs. GFP-ADUK; Student's t-test. **G:** mCherry-Atg8a punctae per cell in genotypes shown in A-E. GFP-ADUK n=9, GFP-ADUK + FIP200 n=7, GFP-ADUK + Atg13 n= 10, FIP200 n=9, Atg13 n=10. ** = p<0. 005 vs. GFP-ADUK, ## = p<0. 005 vs. FIP200; Student's t-test. All larvae raised in well-fed conditions. Nuclei counterstained with DAPI. Scale bar represents 10 μm. Error bars represent standard error.

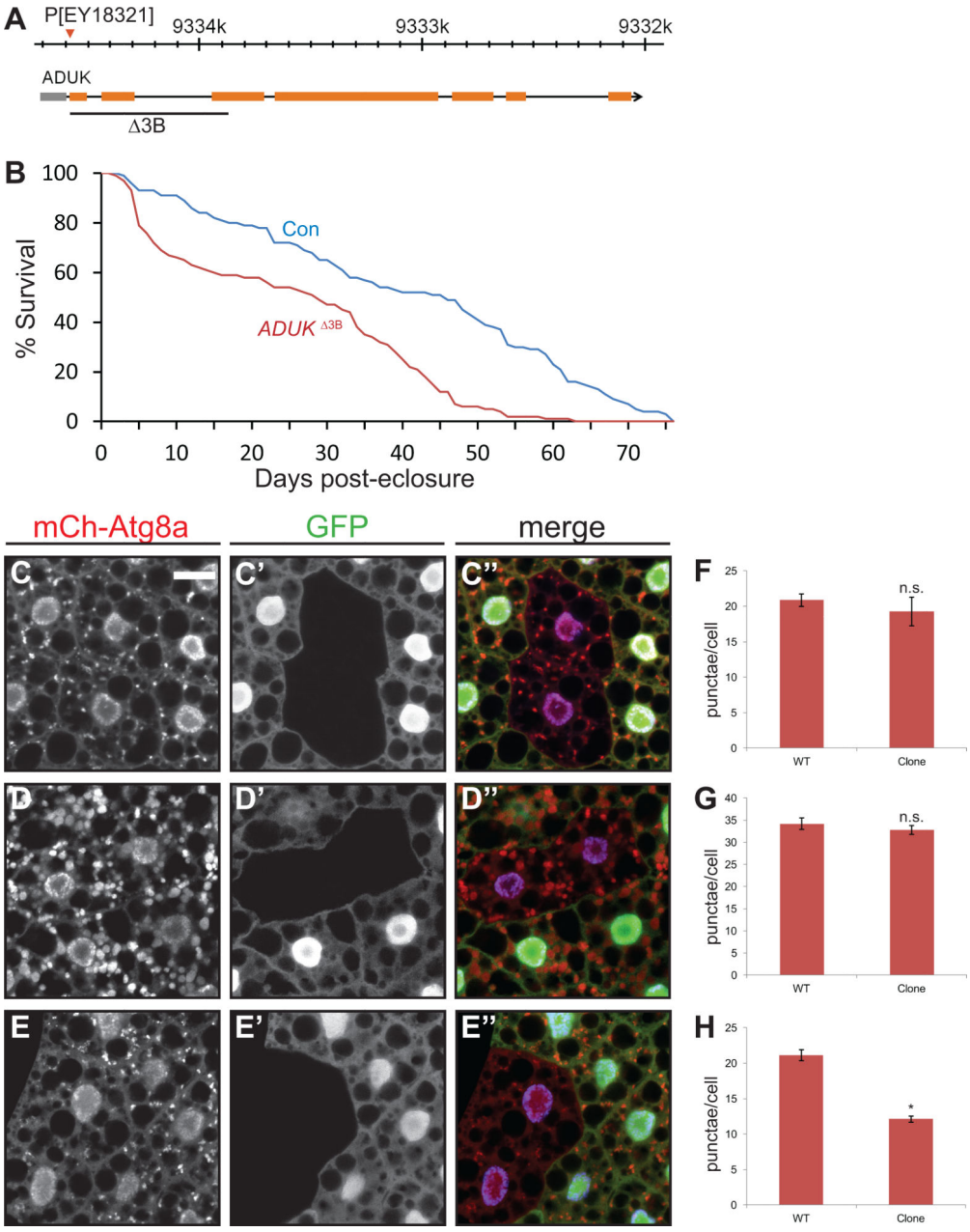

Figure 4. Loss of ADUK reduces adult survival and blunts autophagic response to DMSO

A: Schematic showing the extent of the *ADUK*$^{\Delta 3b}$ deletion. Scale indicates the genomic region on the right arm of chromosome 3. **B**: Animals homozygous for *ADUK*$^{\Delta 3b}$ demonstrate reduced adult survival. **C-E''**: *ADUK*$^{\Delta 3b}$ mutant clones (GFP negative cells) demonstrate normal formation of mCherry-Atg8a-marked autophagic vesicles in response to amino acid starvation (C-C'', quantified in F, n=5) and during wandering stage developmental autophagy (D-D'', quantified in G, n=4) but not in response to 5 hour feeding with food containing 5% DMSO (E-E", quantified in H, n=10). Nuclei counterstained with DAPI. Scale bar represents 20 μm. Error bars represent standard error. n.s. = not significant, * = $p<0.05$; Student's t-test.